HIGH-ENERGY NEUTRONS IN FISSION: CATAPULT NEUTRONS

J. Randrup[(1)], R. Capote[(2)], R. Vogt[(3,4)]
(1) Lawrence Berkeley National Laboratory, CA, USA
(2) Suncoast Data Evaluation, Miami, FL, USA
(3) Lawrence Livermore National Laboratory, Livermore, CA, USA
(4) University of California, Davis, CA, USA

Wonder 2026: 7th edition of the International Workshop On Nuclear Data Evaluation for Reactor Applications, Aix-en-Provence, France, 29 June- July 3, 2026

Chronology of PFNS evaluations

- Before 2015 ALL PFNS evaluations based on neutron emission from FF
- Evaluated data files (in ALL libraries) were based on Los Alamos (Madland-Nix) model

Exception: Mannhart evaluation of ^{252}Cf(sf) PFNS based on experimental data

- **2015-2016: New GLSQ evaluation of ^{235}U(n_{th},f) PFNS** undertaken. The measured spectral-averaged cross sections (SACS) in the ^{235}U(n_{th},f) PFNS of ^{90}Zr(n,2n) was used to adjust the high energy component of the ^{235}U(n_{th},f) PFNS.
  - A.Trkov and RC, Phys. Proc. **64**, 48 (2015).
  - A.Trkov, RC, and V.G. Pronyaev, Nucl. Data Sheets **123**, 8 (2015).
  - RC et al (Technical Report of the IAEA CRP) Nucl. Data Sheets **131**, 1 (2016)

"It doesn't matter how beautiful your theory is,
it doesn't matter how smart you are.
If it doesn't agree with experiment, it's wrong."

Richard Philips Feynman,

Nobel Prize in Physics 1965

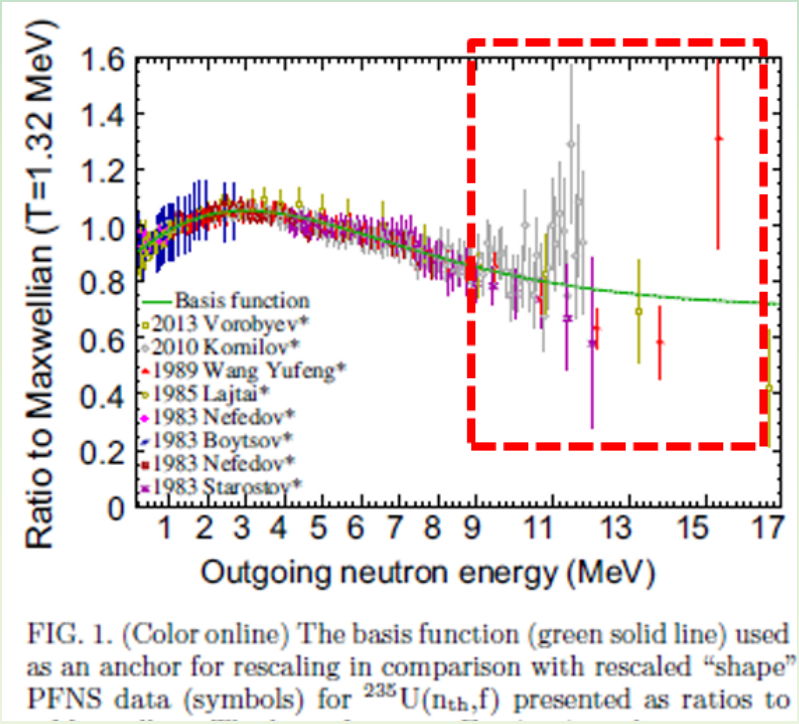

FIG. 1. (Color online) The basis function (green solid line) used as an anchor for rescaling in comparison with rescaled "shape" PFNS data (symbols) for ^{235}U(n_{th},f) presented as ratios to

Roberto Capote, Suncoast Data Evaluation
e-mail: r.capotenoy@yahoo.com

IRDFF validation in ^{252}Cf(sf) reference neutron field

A. Trkov et al, "IRDFF-II: A New Neutron Metrology Library" Nucl. Data Sheets **163**, 1 (2020).

2020

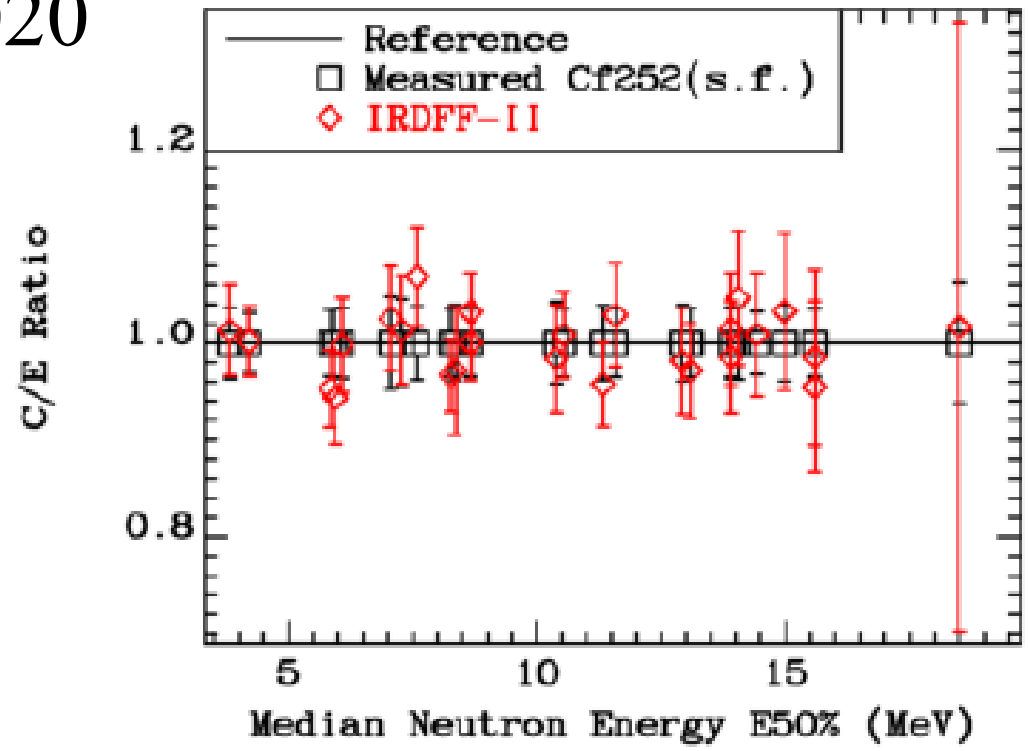

FIG. 123. (Color online) C/E relative to median energy $E_{50\%}$ for the IRDFF-II cross sections averaged in the ^{252}Cf(s.f.) neutron field measured at Řež near Prague. Plotted values are listed in Table 19.

The IRDFF library addresses neutron dosimetry needs for fission and fusion applications for 0<En<60 MeV

The library includes 119 metrology reactions with covariance information (and low uncertainties)

Cross section evaluations validated vs SACS measurements in ^{252}Cf(sf) PFNS

Roberto Capote, Suncoast Data Evaluation
e-mail: r.capotenoy@yahoo.com

Measured SACS ratio in ^{252}Cf(sf) and ^{235}U(n_{th},f) PFNS

(SACS ratio to reduce exper. uncert.)

High-energy neutron emission in thermal neutron-induced fission of ^{235}U

Martin Schulc,[1] Michal Kostal,[1] Roberto Capote,[2] Jan Simon,[1] Evzen Novak,[1] and Tomas Czakoj[1]

2024 PHYSICAL REVIEW C **109**, 054616 (2024)

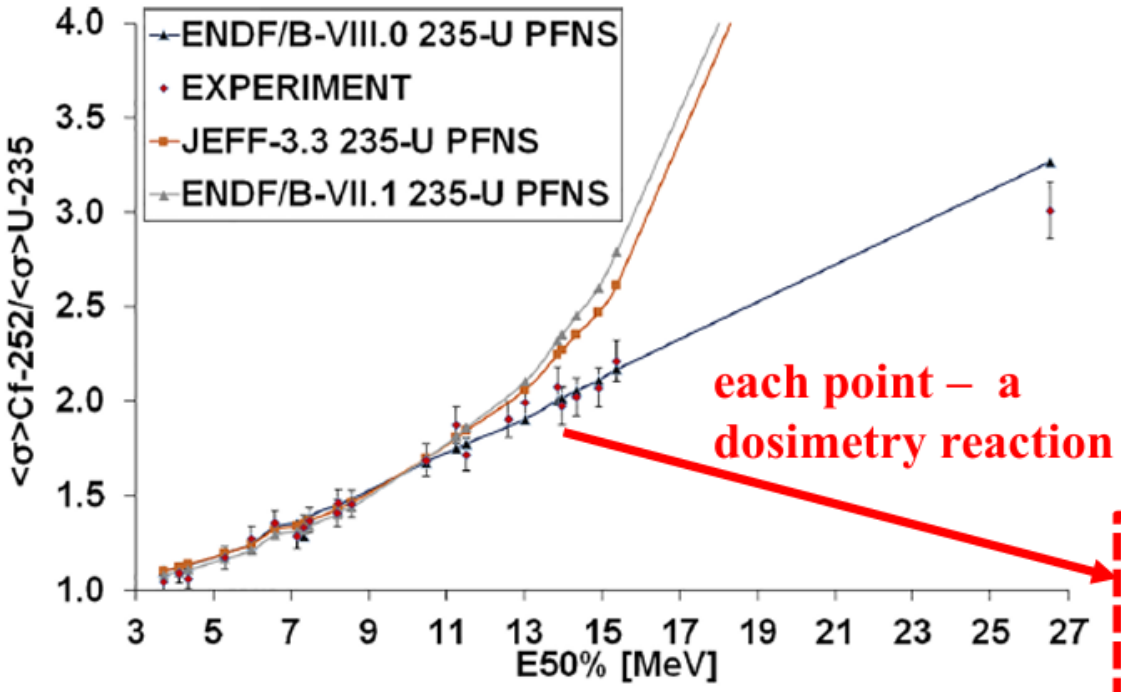

FIG. 3. SACS ratios and uncertainties as a function of the mean neutron response energy $E50\%$ of each dosimetry reaction listed in Table 2.

TABLE II. Mean response neutron energies in MeV for dosimetry reactions and corresponding experimental SACS ratios and their relative uncertainties. ^{169}Tm$(n, 3n)$ was not measured in reactors.

Reaction	$E50\%$ (MeV)	SACS Ratio	Unc. (%)
^{47}Ti$(n, p)^{47}$Sc	3.73	1.042	2.7
^{58}Ni$(n, p)^{58}$Co	4.12	1.088	2.8
^{54}Fe$(n, p)^{54}$Mn	4.36	1.056	2.6
^{92}Mo$(n, p)^{92m1}$Nb	5.29	1.170	2.4
^{46}Ti$(n, p)^{46}$Sc	5.98	1.273	2.9
^{60}Ni$(n, p)^{60}$Co	6.57	1.352	4.2
^{63}Cu$(n, \alpha)^{60}$Co	7.14	1.282	3.2
^{54}Fe$(n, \alpha)^{51}$Cr	7.31	1.327	3.0
^{56}Fe$(n, p)^{56}$Mn	7.46	1.367	2.2
^{24}Mg$(n, p)^{24}$Na	8.19	1.404	2.2
^{48}Ti$(n, p)^{48}$Sc	8.22	1.460	2.8
^{27}Al$(n, \alpha)^{24}$Na	8.56	1.454	2.8
^{197}Au$(n, 2n)^{196}$Au	10.47	1.686	3.7
^{93}Nb$(n, 2n)^{92m1}$Nb	11.26	1.872	2.5
^{127}I$(n, 2n)^{126}$I	11.51	1.715	4.6
^{58}Ni$(n, X)^{57}$Co	12.60	1.900	5.3
^{55}Mn$(n, 2n)^{54}$Mn	13.02	1.990	2.7
^{89}Y$(n, 2n)^{88}$Y	13.84	2.076	2.6
^{19}F$(n, 2n)^{18}$F	13.96	1.973	2.6
^{90}Zr$(n, 2n)^{89}$Zr	14.35	2.022	3.9
^{58}Ni$(n, 2n)^{57}$Ni	14.91	2.070	3.0
^{23}Na$(n, 2n)^{22}$Na	15.37	2.211	4.3
^{209}Bi$(n, 4n)^{206}$Bi	26.54	3.007	9.1

SACS ratio uncert. below ~5%

Except for Bi(n,4n)

Roberto Capote, Suncoast Data Evaluation
e-mail: r.capotenoy@yahoo.com

Measured SACS ratio in ^{252}Cf(sf) and ^{235}U(n_{th},f) PFNS

(SACS ratio to reduce exper. uncert.)

High-energy neutron emission in thermal neutron-induced fission of ^{235}U

Martin Schulc,[1] Michal Kostal,[1] Roberto Capote,[2] Jan Simon,[1] Evzen Novak,[1] and Tomas Czakoj[1]

2024 PHYSICAL REVIEW C 109, 054616 (2024)

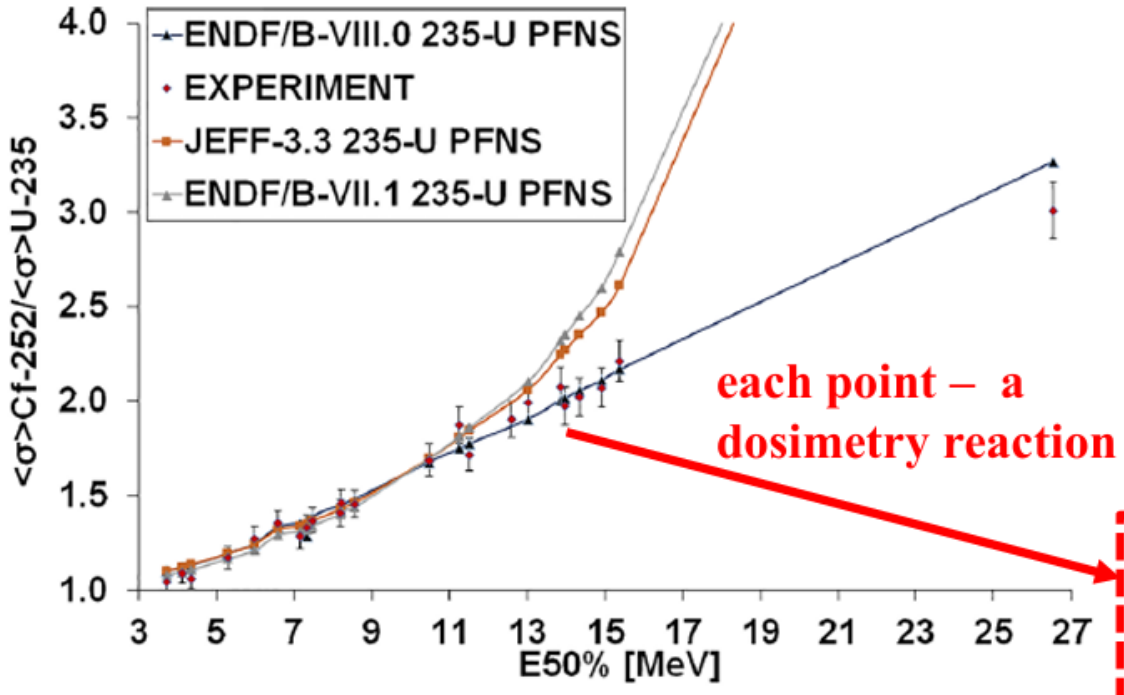

TABLE II. Mean response neutron energies in MeV for dosimetry reactions and corresponding experimental SACS ratios and their relative uncertainties. ^{169}Tm(n, $3n$) was not measured in reactors.

Reaction	$E50\%$ (MeV)	SACS Ratio	Unc. (%)
^{47}Ti(n, p) ^{47}Sc	3.73	1.042	2.7
^{58}Ni(n, p) ^{58}Co	4.12	1.088	2.8
^{54}Fe(n, p) ^{54}Mn	4.36	1.056	2.6
^{92}Mo(n, p) ^{92m1}Nb	5.29	1.170	2.4
^{46}Ti(n, p) ^{46}Sc	5.98	1.273	2.9
^{60}Ni(n, p) ^{60}Co	6.57	1.352	4.2
^{63}Cu(n, α) ^{60}Co	7.14	1.282	3.2
^{54}Fe(n, α) ^{51}Cr	7.31	1.327	3.0
^{56}Fe(n, p) ^{56}Mn	7.46	1.367	2.2
^{24}Mg(n, p) ^{24}Na	8.19	1.404	2.2
^{48}Ti(n, p) ^{48}Sc	8.22	1.460	2.8
^{27}Al(n, α) ^{24}Na	8.56	1.454	2.8
^{197}Au(n, $2n$) ^{196}Au	10.47	1.686	3.7
^{93}Nb(n, $2n$) ^{92m1}Nb	11.26	1.872	2.5
^{127}I(n, $2n$) ^{126}I	11.51	1.715	4.6
^{58}Ni(n, X) ^{57}Co	12.60	1.900	5.3
^{55}Mn(n, $2n$) ^{54}Mn	13.02	1.990	2.7
^{89}Y(n, $2n$) ^{88}Y	13.84	2.076	2.6

SACS ratio uncert. below ~5%

Evaluated ^{235}U(n_{th},f) PFNS in excellent agreement with MEASURED SACS ratios: Excess of non-evaporation neutrons above ~10 MeV. What is the origin? Scission neuts?

Roberto Capote, Suncoast Data Evaluation
e-mail: r.capotenoy@yahoo.com

Scission neutron studies

1) Neck rupture neutrons emitted at scission (~10^{-22} sec)

Scission neutrons suggested very early in fission studies (4 Nobel prizes)

- H.L. Anderson, **E. Fermi**, and H.B. Hanstein, Phys. Rev. 55, 797 (1939).
- **L. Szilard** and W.H. Zinn, Phys. Rev. 55, 799 (1939).
- H. von Halban, **F. Joliot**, and L. Kowarski, Nature 143, 939 (1939)
- **N. Bohr** and J.A. Wheeler, Phys. Rev. 56, 426 (1939)
- …

2) Catapult neutrons emitted just after scission from FFs (~$3x10^{-22}$ sec)

- A. Bulgac et al at CNR*2025, IAEA, Vienna showed a fission movie of the density evolution during scission (calculated using state-of-art TDDFT theory). It was striking how quickly the juxtaposed protrusions healed and that gave Randrup the idea which was implemented in the model described in this presentation:
- J. Randrup, RC, R. Vogt, "Catapult neutrons from neck snapping in fission", **arXiv 2604.10790v1**

- I. Abdurrahman, A. Bulgac, et al Phys. Rev. Lett. **132** (2024) 242501

cited P. Mädler, Catapult Mechanism for Fast Particle Emission in Fission and Heavy Ion Reactions, Z. Phys. **A321**, 343 (1985)

Roberto Capote, Suncoast Data Evaluation
e-mail: r.capotenoy@yahoo.com

TDDFT scission neutron studies

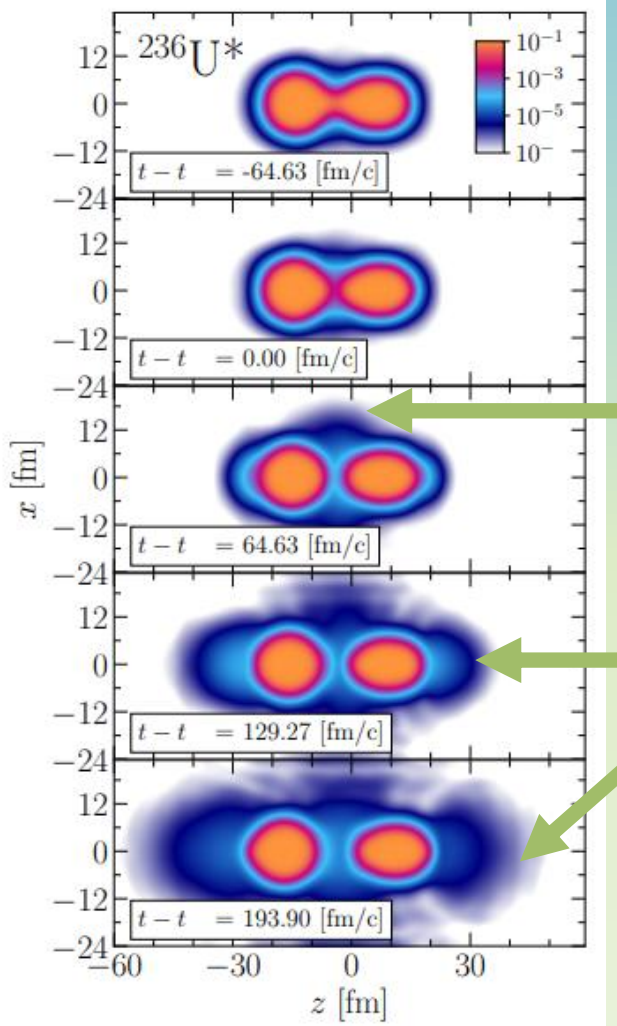

FIG. 1. Time series of the neutron number density in fm^{-3} for a typical fission trajectory.

I. Abdurrahman, A. Bulgac, et al Phys. Rev. Lett. **132** (2024) 242501

Two types of neutrons emitted at scission

1) Neck rupture neutrons (emitted perp. to fiss. axis)

2) + Catapult neutrons (fly in front of the FF along the fission axis, higher-energy spectrum)

The scission neutrons had energies up to 16−18MeV, with a mean energy of ≈3MeV, and their multiplicity was conservatively estimated to be 9 − 14% of the total.

Roberto Capote, Suncoast Data Evaluation
e-mail: r.capotenoy@yahoo.com

Timeline of neutron emission in fission

Stage	Process	Timescale
1	Neck rupture at scission	10^{-22} s
2	Coulomb acceleration	10^{-21}–10^{-20} s
3	Fragment shape relaxation	10^{-20}–10^{-19} s
4	Prompt neutron evaporation	10^{-19}–10^{-16} s
5	Prompt γ emission	10^{-16}–10^{-14} s

Neck rupture + **catapult neutrons**

Current models (evaporation) FIFRELIN, FREYA, GEF, CGMF, …

Scission neutrons (not used in current model codes) and may include:

1) Neutrons emitted at scission at ~10^{-22} sec (neck rupture)
2) Catapult neutrons emitted just after scission from FFs (~3x10^{-22} sec)

Roberto Capote, Suncoast Data Evaluation
e-mail: r.capotenoy@yahoo.com

Modeling of catapult (slingshot) neutrons - I

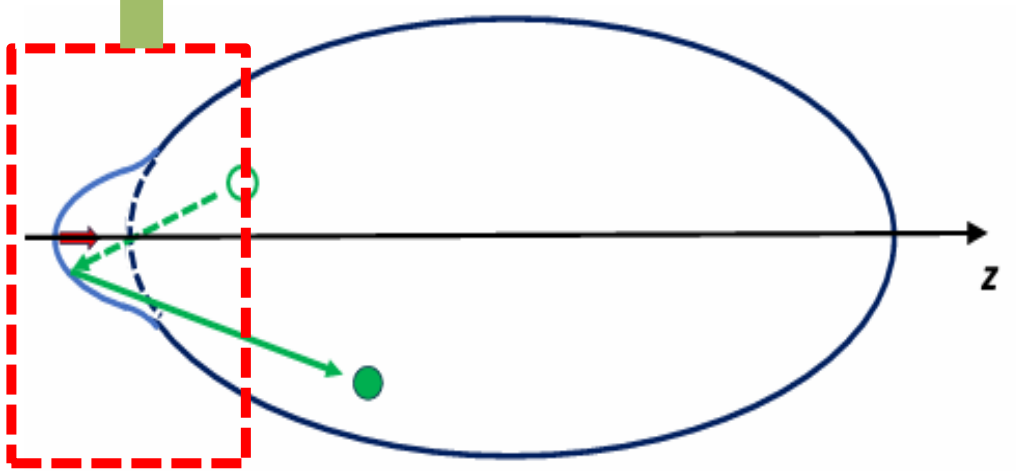

FIG. 1: Shortly after scission the remnant of the ruptured neck endows each fragment with a bulge that is rapidly shrinking towards the smooth reference shape. An approaching nucleon is reflected from the inwards moving bulge surface, thereby being boosted to a higher energy.

In cylindrical coordinates, reference shape c/a=1.8

$$\rho_s^2/a^2 + z_s^2/c^2 = 1$$

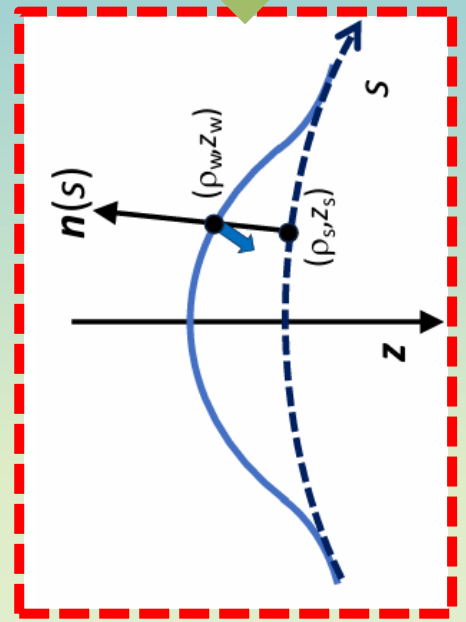

$$h(s;t) = h_0(t)g(s), \quad g(s) = e^{-s^2/2\sigma_0^2}$$

Two parameters h_0, σ_0 describe the bulge

Roberto Capote, Suncoast Data Evaluation
e-mail: r.capotenoy@yahoo.com

Modeling of catapult (slingshot) neutrons - I

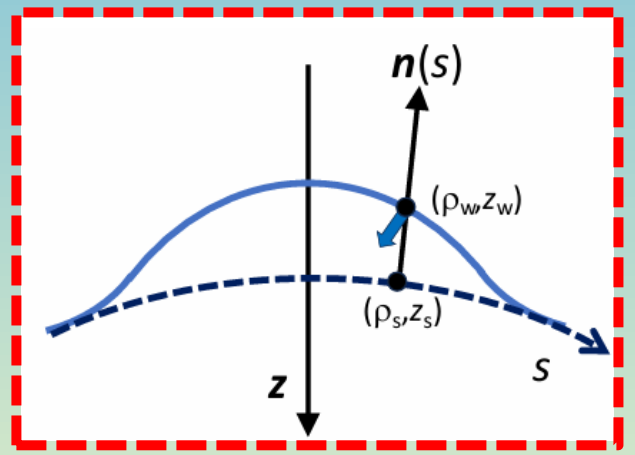

$$h(s;t) = h_0(t)g(s), \quad g(s) = e^{-s^2/2\sigma_0^2}$$

Bulge given by two parameters h_0, σ_0

Bulge shrinks to 5% of its initial value in ~3.4×10^{-22} s

Increase in potential energy due to bulge $V_{\rm bulge}(h_0) = \gamma \Delta S(h_0)$ $\gamma \approx 0.9\,{\rm MeV/fm^2}$

For the FF, it is as if its surface had been pulled out locally and then released (hence the term "slingshot" introduced by Abdurrahman et al in Phys. Rev. Lett. **132** (2024) 242501). Thus, when the neck snaps, the created surface bulge is suddenly being accelerated inwards by a driving force: $F_{\rm drive}(h_0) = -\partial V_{\rm bulge}/\partial h_0$

See more details of the model in J. Randrup, RC, R. Vogt, "Catapult neutrons from neck snapping in fission", **arXiv 2604.10790v1** (under review in PRC)

Roberto Capote, Suncoast Data Evaluation
e-mail: r.capotenoy@yahoo.com

Modeling of catapult (slingshot) neutrons - II

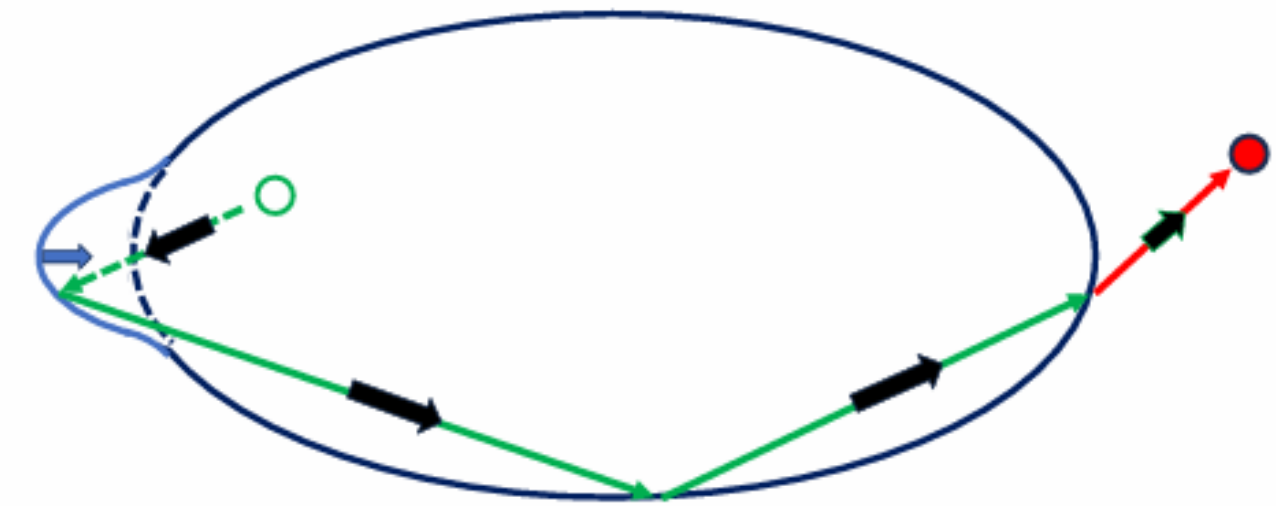

Boosted neutrons may get reflected back from the nuclear surface via elastic scattering **(green)** and eventually may escape **(red)**

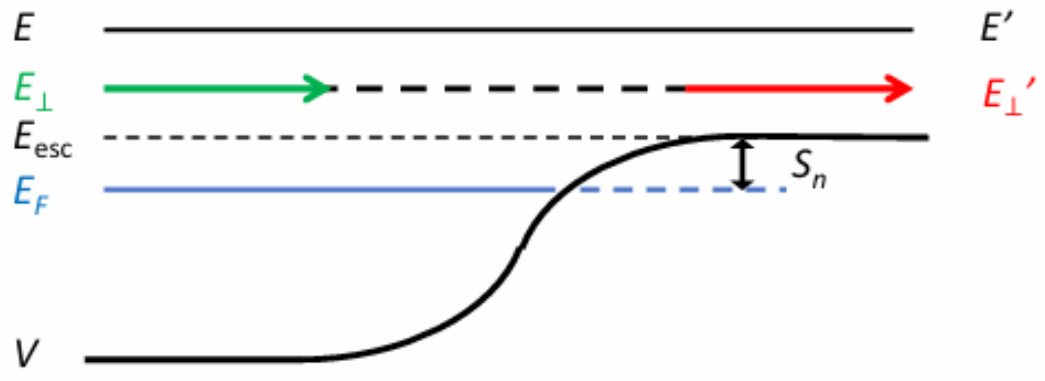

FIG. 4: Illustration of the emission process: At the nuclear surface the effective potential V increases from its bulk value to zero. An unbound neutron has a total energy E above the escape threshold $E_{esc} = E_F + S_n$ and approaches the surface with the normal energy $E_\perp = \frac{1}{2}mv_\perp^2$. If $E_\perp$ also exceeds E_{esc} the neutron is emitted with a reduced normal energy, $E'_\perp = E_\perp - E_{esc}$, while its motion parallel to the surface remains unchanged.

Roberto Capote, Suncoast Data Evaluation
e-mail: r.capotenoy@yahoo.com

Catapult neutrons – results – table

Dependence on bulge σ_0 and h_0

$\overline{\nu}_{cat}$: $\overline{E}_{cat}$	σ_0 =0.8 fm	σ_0 =1.0 fm	σ_0 =1.2 fm
h_0=1.6 fm	2.8: 11.5	3.2: 8.9	3.6: 7.3
h_0 =2.0 fm	3.2: 12.0	3.8: 9.1	4.2: 7.4
h_0 =2.4 fm	3.7: 12.4	4.3: 9.3	4.8: 7.5

TABLE I: The expected number of catapult neutrons per fragment $\overline{\nu}_{cat}$ (times 100) together with their mean kinetic energy $\overline{E}_{cat}$ (in MeV) calculated for various initial bulge heights h_0 and bulge widths σ_0, for fragments having $c/a = 1.8$.

c/a=1.8

Dependence on deformation:

Deformation	<E> catapult [MeV]	ν catapult
c/a=2.0 (more deformed)	9.66	3.3
c/a=1.8 (REF)	9.14	3.2
c/a=1.6 (less deformed)	8.65	3.0
c/a=1.0 (spherical)	7.7	2.7

h_0 = 2.0 fm; σ_0=0.8 fm

Total contribution includes both fragments, likely with different c/a

Roberto Capote, Suncoast Data Evaluation
e-mail: r.capotenoy@yahoo.com

Catapult neutrons relative to FF evaporation

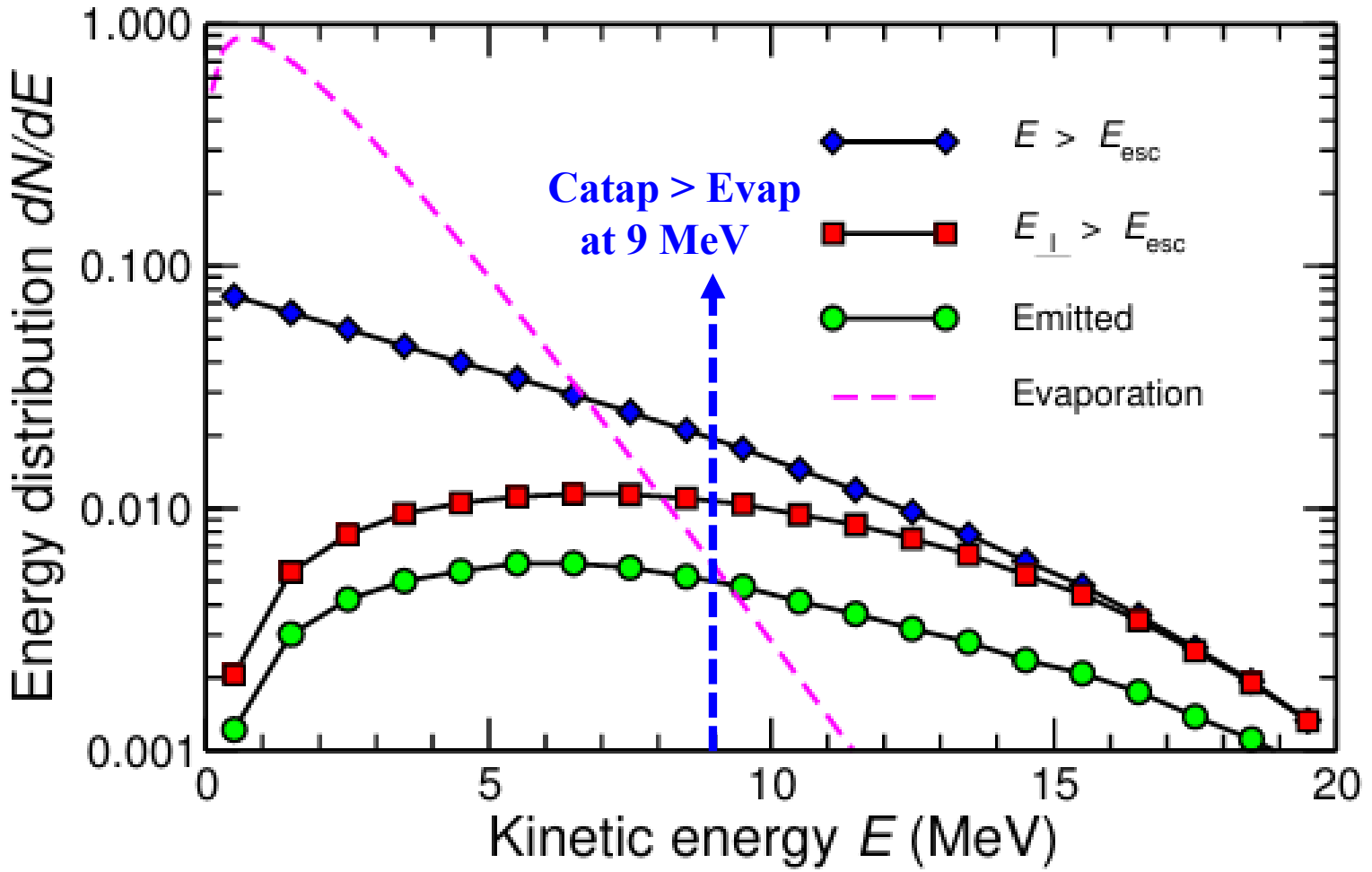

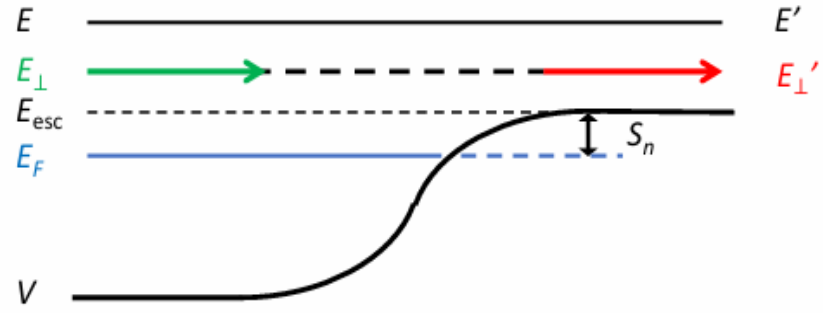

FIG. 4: Illustration of the emission process: At the nuclear surface the effective potential V increases from its bulk value to zero. An unbound neutron has a total energy E above the escape threshold $E_{\rm esc} = E_F + S_n$ and approaches the surface with the normal energy $E_\perp = \frac{1}{2}mv_\perp^2$. If $E_\perp$ also exceeds $E_{\rm esc}$ the neutron is emitted with a reduced normal energy, $E'_\perp = E_\perp - E_{\rm esc}$, while its motion parallel to the surface remains unchanged.

Roberto Capote, Suncoast Data Evaluation
e-mail: r.capotenoy@yahoo.com

Summary and conclusions

- The catapult neutron emission mechanism is universal, and exhibit weak energy dependence

- The dependence on the specific fission fragment is relatively moderate, though some general trends appear. Thus, for a given initial bulge height, a wider bulge increases the multiplicity but hardly affects the energy, while a higher initial bulge, for a given bulge width, increases both the multiplicity and the energy. This finding supports the speculation by Mädler that fission events with lower TKE (and hence a more elongated neck) will produce more energetic catapult neutrons.

- Catapult neutrons exist (as suggested by Mädler in 1975), at the level of a few percent. They have energies far in excess of typical evaporation neutrons, a key characteristic that should make it easier to identify them experimentally.

- The calculations support the conclusion of Schulc et al. - Phys Rev **C109** (2024) 054616 that very energetic neutrons are emitted during fission, and their finding that the measured neutron spectrum dominates over the standard evaporation spectrum above ≈10 MeV is consistent with our results.

- Further TDDFT studies are encouraged to confirm our theoretical results.

Roberto Capote, Suncoast Data Evaluation
e-mail: r.capotenoy@yahoo.com

THANKS FOR YOUR ATTENTION !

Basic concepts: SACS in spectrum

SACS-Cf = SACS in Cf-252(sf) PFNS

$$SACS = \frac{\int \sigma(E)\varphi(E)dE}{\int \varphi(E)dE} \qquad \int_n \varphi(E)dE \equiv 1$$

$$SACS = \int \sigma(E)\varphi(E)dE \cong \sum_{k=0} \varphi(k)\sigma(k)$$

$$\frac{\partial(SACS)}{\partial\sigma(k)} = \varphi(k)$$

SACS sensitivity to $\sigma(k)$ = spectral weight $\varphi(k)$ @ E_k

SACS are VERY CLEAN INTEGRAL DATA

Roberto Capote, Suncoast Data Evaluation
e-mail: r.capotenoy@yahoo.com